Applied Water Science (2022) 12:179
https://doi.org/10.1007/s13201-022-01700-9

ORIGINAL ARTICLE

Adsorption characteristics of methyl red dye by Na_2CO_3-treated jute fibre using multi-criteria decision making approach

Amit Kumar Dey[1] · **Abhijit Dey**[2] · **Rumi Goswami**[3]

Received: 2 September 2021 / Accepted: 20 May 2022 / Published online: 14 June 2022

Abstract

This article reports the use of sodium carbonate-treated jute fibre (SCTJF), for the removal of an azo dye methyl red (MR). Face-centred CCD, based on RSM, experimental design has been used to acquire a definite number of experimental paths in order to ascertain improved experimentation towards reaching performance characteristics that are ideal in order to remove the dye (MR) dissolved in aqueous solution. Independent variable parameters used for dye removal and maximum adsorption capacity (Q_{max}) are: rotational speed (100 RPM, 150 RPM and 200 RPM), temperature (293 K, 303 K and 313 K), pH (3, 7 and 11) and adsorbent (SCTJF) dose (10 mg/L, 14 mg/L and 18 mg/L), where Q_{max} of the treated jute was considered to be the performance measure for dye removal. ANOVA was used in conjunction with a quadratic model of second order to explore the impact of operating variables and their elucidation. pH = 7.08, temperature = 299.57 K, SCTJF dose = 14.74 g/L, and stirring speed = 155 RPM were found to be the best process conditions. With a desirability of 0.98, the computed experimental Q_{max} (32.11 mg/g) and anticipated Q_{max} (31.7 mg/g) were in resonance within the domain threshold, indicating outstanding accuracy of the experimentation operations.

Keywords Adsorption · Desorption · Kinetics · Thermodynamics · CCD · RSM · Na_2CO_3 treated jute fibre (SCTJF) · Methyl red

Introduction

Dyes are difficult to break because of their complex bonding structure and hence poses major environmental and health risks. In addition to other consequences, certain dyes have been discovered to have mutagenic and carcinogenic properties (Dey and Kumar 2017a; Dey et al. 2018). Dyes are generally split into two categories based on the source of the material: synthetic dyes and natural dyes. The bulk of vegetable dyes, also known as natural colours, are derived from plant sources such as roots, berk, berries, leaves, and wood (Dey and Dey 2021a). They are quickly biodegradable and are eco-friendly. Synthetic dyes, on the other hand, are used in practically every colour applicable industries we see today (Aksakal and Ucun 2010a).

Textile industry effluents can contain a significant quantity of synthetic azo dye content. The environmental and health hazards associated with dye generated by textile businesses are becoming a focus of scientific research. Researchers have used a variety of techniques to effectively remove colour from wastewater bodies, depending on the approach. Membrane separation, biological oxidation treatment, coagulation-flocculation, ultrasonic irradiation, coagulation-flocculation, photocatalysis and ozonation are some of the procedures (Dey and Kumar 2017b; Kumar et al. 2012; Chen and Zhang 2014; Chiang 2008; Cho and Joh 2007; Chong et al. 2009; Chowdhury et al. 2011; Chowdhury and Saha 2010a). Among various materials and methods, the combination of use of activated carbon (AC) and adsorption is among the most effective ways with the ability to remove such quantity of dye from the aqueous solution that can be practically applicable. However, AC has its own set of limitations, including a high initial cost of manufacture, complications in regeneration after depletion, and a reduction in removal effectiveness upon regeneration (Reddy and

✉ Amit Kumar Dey
ak.dey@cit.ac.in

[1] Department of Civil Engineering, Central Institute of Technology Kokrajhar, Kokrajhar, Assam 783370, India

[2] Department of Mechanical Engineering, National Institute of Technology Srinagar, Srinagar, J&K 190006, India

[3] PhD Scholar, Dept. of Civil Engineering, Central Institute of Technology Kokrajhar, Kokrajhar, Assam 783370, India

Yun 2016; Crini et al. 2007). As a result, today's researchers are emphasising the use of adsorbents that are cost-effective, eco-friendly, and available in abundance (Freundlich 1906; Ganguly and Chanda 1994; Gupta et al. 2013; Ho and McKay 1999). In our study, a low-cost bio-sorbent, Na_2CO_3-treated jute fibre (SCTJF) was used for removing methyl red (MR) dye via the adsorption method. Jute is an essential crop in the Indian subcontinent and is one of the numerous agricultural products in India. Almost 85% of the world's jute production is generated in India and Bangladesh. Cellulose, hemicellulose, lignin, and other low molecular weight hydrocarbons are the main components of jute fibre (Ibrahim et al. 2010). These elements, which have hydroxyl and carboxyl functional groups, are the driving forces behind dye adsorption onto the adsorbent. According to a literature review, researchers have successfully removed dye using several surface modified low-cost bio-sorbents (Kumar et al. 2012; Kansal et al. 2007; Kapdan and Ozturk 2005; Koch et al. 2002). Recently, the focus has shifted to adsorbent surface modification in order to use it more effectively than activated carbon to make waste water free from hazardous colours. The purpose of modification of surface is to increase the percentages of important functional groups on the adsorbent surface, such as sulphate, hydroxyl, carboxylate, carboxyl, and phosphate groups (Lagergren 1898). When it comes to dye removal, researchers are not confined to using simply experimental models; various mathematical models and software programmes are available that are used to study and determine the ideal circumstances needed for the intended result. Several studies have already been conducted in this field, such as the use of response surface methodology (RSM) to improve process factors to remove dye using a new adsorbent (Langmuir 1916). RSM is used in the present analysis to investigate the removal of methyl red dye using a low-cost adsorbent. For regression analysis and optimization of the removal of colour from aqueous dye solution using a novel adsorbent, statistical designs and surface plots are utilised (Liang et al. 2010; Liu and Liu 2008). Central composite design (Malik and Saha 2003; Munagapati and Kim 2016) was used to examine modelling and optimization for azo dye (methyl red) degradation using RSM.

RSM is used to evaluate the rapport when the input parameters are quantitative. In addition, the variables (X_1 and X_2) maximise the outcome of the system (Y). In short, the variables influence the system outcome as expressed below (Taweel and Gouda 2010):

$$y = f\left(X_1, X_2\right) + \varepsilon. \tag{1}$$

Indeed, RSM manipulates the precise design of experiments (DoE), which has recently acquired favour for formulation. Besides, its statistical approach is used to evaluate the interaction effect between the process factors then the traditional approach (Adsorption of anionic Myers R et al. 1989).

Indeed, RSM is expedient in creating and analysing the system, as the ultimate aim is to optimise the impact response by several factors. RSM is a scientific and computational technique for modelling and analysing the scenarios that consider various factors that affect the desired output and attempt to maximise the final outcome (Dey and Dey 2021b). Relation between the dependent and the independent variables is unknown in most of the RSM cases (Dey and Pandey 2018a). So, in RSM, estimation for the set of independent variables 'X' is done first and then the desirable output 'Y' is calculated. In several portions of the response variable, a low-order polynomial is used generally. The functional approximation in the first-order model is well represented by the independent parameters and is given as (Dey and Dey 2021b):

$$y = \beta_0 + \beta_1 x_1 + \beta_2 x_2 + \ldots + \beta_k x_k + \varepsilon. \tag{2}$$

A regression model is also known as a polynomial quadratic model of order two as shown in Eq. (3) which shows the system quality characteristic. The software 'Design Expert 11.0' gives an approximation of the regression model coefficient (Dey and Dey 2021b). When the structure is having curvature in the second-order form, a higher-order polynomial is used as (Dey and Pandey 2018a):

$$y = \beta_0 + \sum_{i=1}^{k} \beta_i x_i + \sum_{i=1}^{k} \beta_{ii} x_i^2 + \sum_{i<j} \sum \beta_{ij} x_i x_j + \varepsilon. \tag{3}$$

RSM technique can forecast the influence of process variables on performance that attributes in a better way and therefore be deemed a better optimization alternative (Munagapati and Kim 2016). As a result, the experimental design is based on RSM's face-centred central composite design (CCD). The goal of this study is to use a mathematical model to analyse the maximum sorption capacity. (Q_{max}) of Na_2CO_3-treated jute fibre (SCTJF) to eliminate methyl red (MR) and to use RSM to examine the effect of process parameters and their performance requirements. Using the RSM technique, mathematical models (quantitative) are also employed to investigate the effects of temperature, pH, SCTJF dosage, and RPM on adsorption capacity (Mustafa et al. 2014).

Jute is a multi-component, multicellular fibrous substance with a good cellulose content. Apart from a high amount of α-cellulose (~ 60%), hemi-cellulose (~ 23%) and lignin (~ 14%) are the two other significant chemical elements found in jute, as well as traces of fat and

wax. Researchers infers that an ester bond forms between sections of hemicellulose and lignin that are chemically linked by lignin's hydroxyl groups and hemicellulose's carboxyl groups (Namasivayam and Sureshkumar 2006). The presence of carboxyl and hydroxyl groups on the outer surface of adsorbent is the primary cause for adsorption of dyes from aqueous media. In this research, adsorbent was prior treated with Na_2CO_3, which is consistent with the most often used chemical treatment technique for surface treatment of cellulose-based materials, namely alkali treatment to improve sorption capabilities of any adsorbent which is not in activated carbon form (Ndazi et al. 2007). The covalent bond between the components of ligno cellulosic material is also destroyed by treating the jute fibre with an aqueous sodium carbonate (Na_2CO_3) solution, which hydrolyses depolymerising lignin and hemicellulose. The treatment alters the morphological molecular and super molecular characteristics of cellulose, resulting in changes in pore structure, stiffness, crystallinity accessibility, unit cell structure, and fibril orientation (Panswad and Wongchaisuwan 1986). Washing with Na_2CO_3 improves some of the features of cellulose, such as reactivity, natural ion-exchange capacity, and structural stability. Alkali treatment, which removes waxes and natural lipids from the cellulose fibre surface, identifies some of the chemically reactive functional groups, such as –OH (Ravikumar et al. 2007). Rice husk (high in cellulose compounds) treated with alkali (NaOH) has previously seen to be influential as an adsorbent for removing azo dyes from aqueous solutions (Ravikumar et al. 2005). Hence, from the literature review, it was revealed that components like cellulose and hemicellulose are abundant in jute fibres, and methyl red is essentially an azo dye; the feasibility of employing (alkali treatment) Na_2CO_3-treated jute fibre (SCTJF) to remove methyl red from aqueous solution was investigated in this study. Also, the goal of the analysis was to validate the dye adsorption experimental results with the help of mathematical modelling like RSM. Analysis will be done to check the feasibility and efficacy for the removal of an anionic azo dye methyl red (MR) using chemically (Na_2CO_3) modified jute fibre with the aid of adsorption technology using composite design face-centred central (CCD) RSM.

After extensive literature review, the authors understood that although there are numerous studies reported on the use of adsorption to remove synthetic dyes, till now no study has been done on removal of methyl red dye using modified/treated jute fibre. Hence, this gives the authors an opportunity to take up this analysis which at the same time justifies the novelty of the work.

Methods and materials

Jute that had been naturally sun-dried was purchased from the market and cut into 1-mm pieces before being distilled washed and dried again at 60 °C. The acquired sample was then treated for 4 h at 27 °C with 0.01 M Na_2CO_3. The sample was then distilled and rinsed to eliminate any chemicals present in excess in the fibre (if any), and the pH was corrected to 7.0 using 0.1 M NaOH or 0.1 M HCl, before being maintained in a container for 24 h after drying at 100 °C. The adsorbent was the final sample, which was treated with Na_2CO_3 and referred to as sodium carbonate-treated jute fibre (SCTJF) (Dey and Kumar 2017b; Lataye et al. 2008). The adsorbate was an azo dye called methyl red, which has a strong, albeit apparently noncovalent, affinity for cellulose fibres and has the chemical formula $C_{15}H_{15}N_3O_2$ with a molar mass of 269.304 g/mol. Dye was obtained from HiMedia, which is of the Analar grade. A stock dye solution (1000 mg/L; pH 7.0) was produced using double distilled water to begin the experiment.

Surface morphology and characterization of SCTJF

Using a Scanning Electron Microscope (SEM) (MODEL: JSM-6360, JEOL), the surface characteristics of virgin SCTJF and MR dye adsorbed SCTJF were examined under the following conditions: resolution: 3 nm in the secondary electron mode, distance of 8 mm, acceleration voltage of 30 kV, accelerating voltage: from 1 to 30 kV in 1 kV steps, accelerating voltage: from 1 to 30 kV in 1 kV steps, accelerating voltage: from 1 to 30 kV in 1 kV steps, accelerating voltage: from 1 to 30 kV in 1 kV steps, accelerating voltage: from 1 to 30 K.

Fourier transform infrared (FTIR) analysis is a useful approach for characterising and recognizing the functional groups accountable for adsorption. The influence of functional groups for the adsorption of MR dye onto adsorbent surfaces is confirmed by the FTIR spectra. FTIR analysis was done at IIT Bombay SAIF research facility. The study's instrument has the following specifications ((make: Bruker, Germany); model: Hyperion Microscope 3000 with Vertex 80 FTIR System).

Adsorption capacity and percentage removal

The goal of the project was to estimate the maximal MR sorption capacity (Q_{max}) using Na_2CO_3-treated jute fibre. According to the mass balance concept upon the concentration of dye, the amount of maximum adsorbed dye per

unit adsorbent (milligram (mg)) dye adsorbed per gram (g) of adsorbent was determined using Eq. 4:

$$Q_e = \frac{(c_i - c_f)}{m} V \tag{4}$$

where Q_{max} = maximum adsorption capacity (mg/g).
C_i = dye initial concentration in solution (mg/L).
C_f = dye final concentration in solution (mg/L).
V = solution volume (L).
m = adsorbent weight (g).

The following equation was used to calculate the proportion of dye that was eliminated (%):

$$Dye\ removal\ percentage\ (\%) = \frac{(C_i - C_e)}{C_i} \times 100 \tag{5}$$

where C_e = remaining concentration of dye in solution at equilibrium (mg/L).

Isotherm studies related to sorption

Studies for various isotherms related to sorption are the fundamental procedures for determining the adsorption relationship for adsorbent-adsorbate interaction. Isotherms give information about the homogeneous or heterogeneous nature of attraction during the adsorbent–adsorbate interaction as well as the favourability of adsorption. The feasibility of the process of MR dye adsorption onto the SCTJF was investigated in this study utilising two basic nonlinear isotherm equations, namely the Langmuir (1916) and Freundlich (1906) isotherm models, as shown in Eqs. 6 and 8, respectively.

$$\text{Langmuir isotherm model}: q_e = \frac{q_m bCe}{1 + bCe} \tag{6}$$

where q_e = dye adsorbed at Ce (mg/g).
q_m = maximum monolayer sorption capacity, not dependent of temperature.
b = Langmuir adsorption constant, dependant of temperature (L/mg).
Ce = remaining concentration of dye in solution at equilibrium (mg/L).

After analysing the value of unitless constant separation factor (R_L) (Webi and Chakravorty 1974), which can be derived by Eq. 7 and after that, based on the appropriateness of adsorption as to whether the sorption characteristics are linear or inappropriate, the character of the Langmuir isotherm could be anticipated. The nature of the isotherm is revealed by the R_L value, which stipulates as to whether the adsorption process is favourable ($R_L < 1$), unfavourable ($R_L > 1$), linear ($R_L = 1$), or irreversible ($R_L = 0$).

$$R_L = \left(\frac{1}{1 + bC_0}\right) \tag{7}$$

where C_0 = initial dye concentration in the solution (mg/L).

The present work examines an empirical equation, the Freundlich (Freundlich 1906) isotherm equation, which depicts the diversity of the adsorbent's surface during adsorption.

$$\text{Freundlich}: q_e = K_f Ce^{1/n} \tag{8}$$

where K_f and $1/n$ are the system Freundlich abiding attributes.

Ce = remaining concentration of dye in solution at equilibrium (mg/L).

q_e = adsorption capacity at equilibrium (mg/g).

The adsorption capacity and intensity are denoted by K_f and n, respectively. If K_f value increases with an increase in temperature, the reaction is ought to be endothermic; and if K_f value falls with an increase in temperature, the reaction is supposed to be exothermic. The adsorption type is indicated by the other Freundlich constant, $1/n$. When the condition is $0 < 1/n < 1$, process of adsorption is considered to be conducive, again if, $1/n = 1$, sorption condition ought to be irrevocable, and finally, if the condition is $1/n > 1$, in that case adsorption process is said to be unfavourable (Chen and Zhang 2014).

Adsorption kinetic modelling

The sorption system kinetic parameters were then determined using time-dependent experimental findings. Using pseudo-first-order (Lagergren 1898) and pseudo-second-order (Ho and McKay 1999) kinetic models, the rate constant and optimum sorption capacity at various temperature ranges were determined.

$$\text{Pseudo - first order}: q_t = q_1\left[1 - \exp\left(-k_1 t\right)\right] \tag{9}$$

$$\text{Pseudo - second order}: q_t = \frac{q_2^2 k_2 t}{1 + q_2 k_2 t}. \tag{10}$$

Because the preceding kinetic models have a constraint when it comes to determining the sorption process' diffusion mechanism, the rate-controlling phases were determined using an intra-particle diffusion model.

$$\text{Intra - particle diffusion}: q_t = k_i t^{0.5}. \tag{11}$$

For the sorption of MR onto SCTJF, activation energy (E_a) was calculated using the Arrhenius equation. The following is the equation for the same:

$$\ln k = \ln A - \frac{E_a}{RT}. \tag{12}$$

The activation energy E_a can be determined by producing a graph of *ln K vs. 1/T* and looking at the slope of the graph, where T is the temperature in kelvin, and K is either the pseudo-first-order rate constant or the pseudo-second-order rate constant, both of which are based upon sorption rate preferred in the kinetic reaction. The type (physical or chemical) of adsorption is revealed by activation energy. Some thermodynamic parameters, such as ΔG° = change in Gibbs free energy, ΔH° = change in enthalpy, and ΔS° = change in entropy, were examined to determine the adsorption temperature favourability, whether the sorption process is endothermic or exothermic, and whether the sorption process is entropy or enthalpy operated. The analyses were carried out using the equations shown below:

$$\Delta G^\circ = -RT \ln K_{ad} \tag{13}$$

$$K_{ad} = \frac{C_0 - C_e}{C_e^n} \tag{14}$$

$$\Delta G^\circ = \Delta H^\circ - T\Delta S^\circ. \tag{15}$$

The graph of ΔG° *vs.* T was used to determine the values of ΔH° and ΔS°, where C_o is the initial dye concentration in the solution and C_e is the dye concentration in the solution at equilibrium. At equilibrium, $K_{ad}$is the rate constant of the adsorption process. The n value is determined via rate kinetic analysis, which involves determining which rate model best fits the observed data (Aksakal and Ucun 2010a).

Batch experimental procedure

A stock dye solution of 1000 mg/L was prepared initially; henceforth, solutions with concentrations 50 mg/L, 100 mg/L, 150 mg/L and 200 mg/L were calibrated and were considered for the overall analysis. The goal of this study was to fix a dye concentration (say 50 mg/L) and determine the maximum sorption capacity (Q_{max}) as a function of the pH, SCTJF dosage, temperature, and rotational speed input process parameters (RPM). Adsorption analysis was performed batch by batch to investigate the removal of MR dye using the aforementioned procedure parameters. Let's go over the details of the experiment to see how a change in pH affects the final result (Q_{max}). The pH range used in the study was (3–11). The initial pH was calibrated to 3.0, the initial SCTJF dose was 10 g/L, the initial temperature was 293 K, and the rotary shaker was adjusted with a stirring speed of 100 RPM for 200 ml of dye solution with 50 mg/L dye concentration. A rotary incubator was used to regulate the temperature. After that, the solution was allowed to agitate for 5 min each before samples were taken to determine the concentration of the sample solution (after 5 min, 10 min, 15 min and so on up to 180 min). After 120 min of agitation, adsorption was no longer time dependent (equilibrium time). The dye concentrations were calculated using UV/VIS spectroscopy absorbance values with maximum absorbance at a wavelength of 425 nm (λ_{max} = 425 nm). The data were then used to compute Q_{max} (mg/g), the highest quantity of dye adsorbed. Keeping the other process parameters constant, comparable experiments were carried out with different pH values. Similarly, when the pH variation study was completed, other parameters were investigated set-wise by modifying the parameter whose effect was to be determined while leaving the other variables constant.

SCTJF dose (10 g/L, 14 g/L and 18 g/L), temperature (293 K, 303 K, and 323 K), and rotational/stirring speed (100 RPM, 150 RPM, and 200 RPM) were used to evaluate additional parameters. Using 0.1 M HCl or 0.1 M NaOH, pH values were kept in the range of 3–11 for each set of solutions. Experiments were carried out to see if the MR dye could be absorbed by the container walls in the absence of jute. There was no evidence of deterioration or MR dye absorption on container sides. Duplicate tests were run, and mean values were taken into account. All feasible combinations for all process variables were tested using the same set of experiments.

Results and discussion

The elimination of dye from aqueous solution as a function of contact time is represented by a time decay curve. It is determined by measuring the decrease in dye concentration caused by adsorbent removal from a solution over time. Figure 1 depicts the time decay curve for removing MR using SCTJF as the adsorbent at 50 mg/L initial dye concentration, 14 g/L SCTJF dosage, pH 7.0, 150 RPM rotational speed, and 303 K temperature. In adsorption,

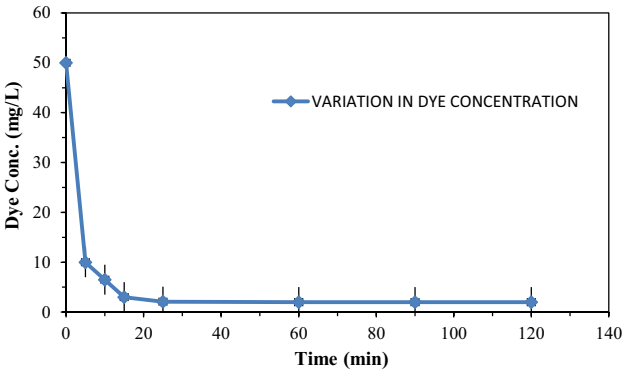

Fig. 1 Time decay curve for the adsorption of MR onto SCTJF

equilibrium time is reached when there is no further substantial adsorption of dye onto the adsorbent beyond a certain time point, or in other words, adsorption of dye is no longer a time-dependent event, as can be seen from the time decay curve.

The rate of adsorption for the adsorbent–adsorbate interaction was rapid during the first 20–25 min. As shown in Fig. 1, it can be observed that within the first 20–25 min, dye concentration in the solution reduced from initial concentration of 50 mg/L–1.2 mg/L. After that, the adsorption rate dropped dramatically. The adsorption site availability is attributed to the fast rate of dye elimination in the early phases. As time passed, the adsorbate–adsorbent interaction intensified, resulting in adsorption site saturation as more dye molecules adsorb onto the sites, resulting in a decrease in the number of adsorption sites and, as a result, a drop in sorption. The equilibrium time for the given investigation was 120 min with a solution concentration of approximately 1 mg/L. Beyond that the adsorption process was no longer dependent on time, similar investigation is carried out earlier also (Dey and Dey 2021a).

Surface morphology and characterization of SCTJF

Figure 2a depicts virgin SCTJF, while Fig. 2c depicts MR adsorbed SCTJF. It can be seen in Fig. 2c that there are numerous MR dye particles attached to the SCTJF surface. Corresponding EDAX images are shown in Fig. 2b and d, respectively. It can be observed from EDAX elemental analysis (Fig. 2b) that, before adsorption, only C, O and Na elements were present on the sorbent surface, after adsorption (Fig. 2d), Cu components were also noticed on the sorbent surface justifying the sorption phenomena. Both the figures are of 1 µm and × 10,000 resolution. Similar results have been reported in earlier research (Dey and Kumar 2017a; Dey et al. 2018; Dey and Dey 2021a).

Figures 3a, and b shows the FTIR spectra of virgin SCTJF and methyl red (MR)-loaded SCTJF, respectively. Due to the constrained hydroxyl or amine groups, the broad and strong band was seen at 3437.84 cm^{-1}. Due to the–CH asymmetric stretching, the next high value of 2914.16 cm^{-1} was observed. The carboxyl group stretching vibration has a wave number of 1741.80 cm^{-1}. The bands at 1640.06 cm^{-1}, 1507.77 cm^{-1}, and 1460.99 cm^{-1} were used to assign asymmetric and symmetric

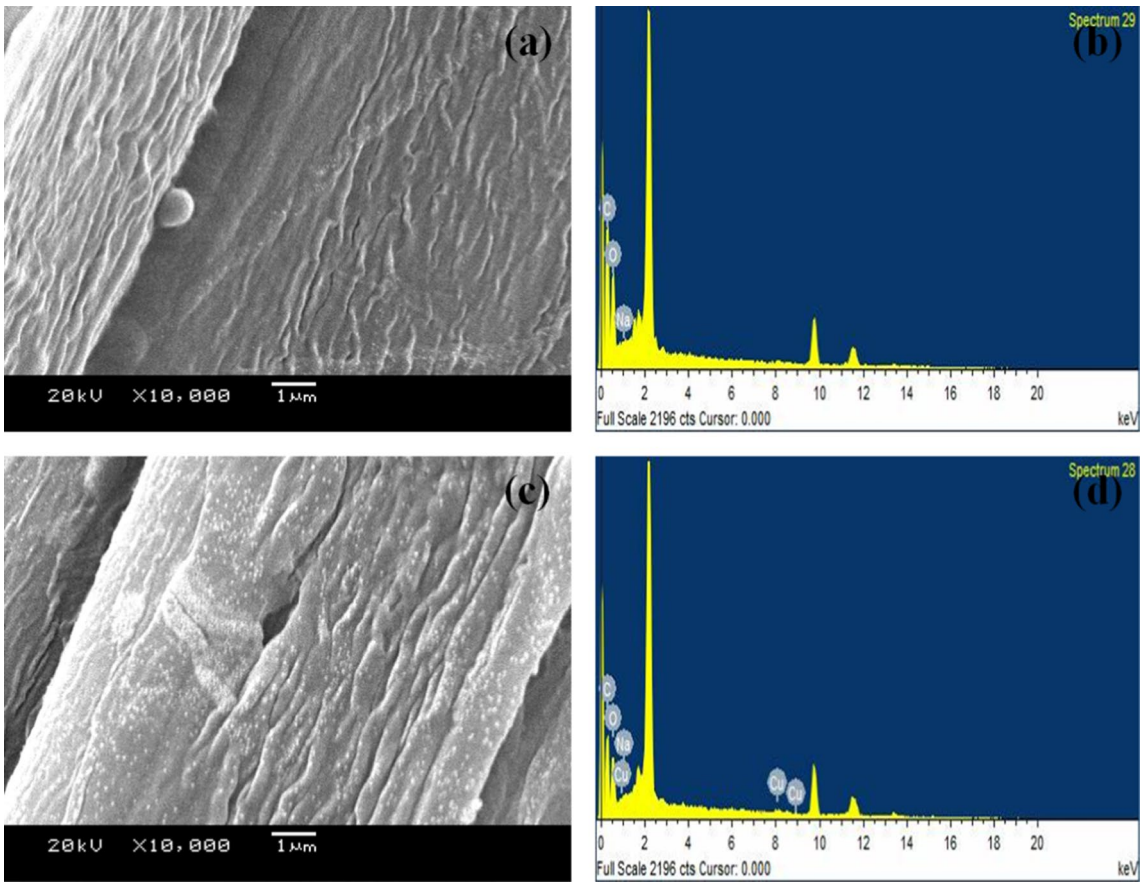

Fig. 2 **a** SEM image of SCTJF before adsorption; **b** SEM image of SCTJF after MR dye adsorption; **c** EDAX image of SCTJF before adsorption; **d** EDAX image of SCTJF after MR dye adsorption

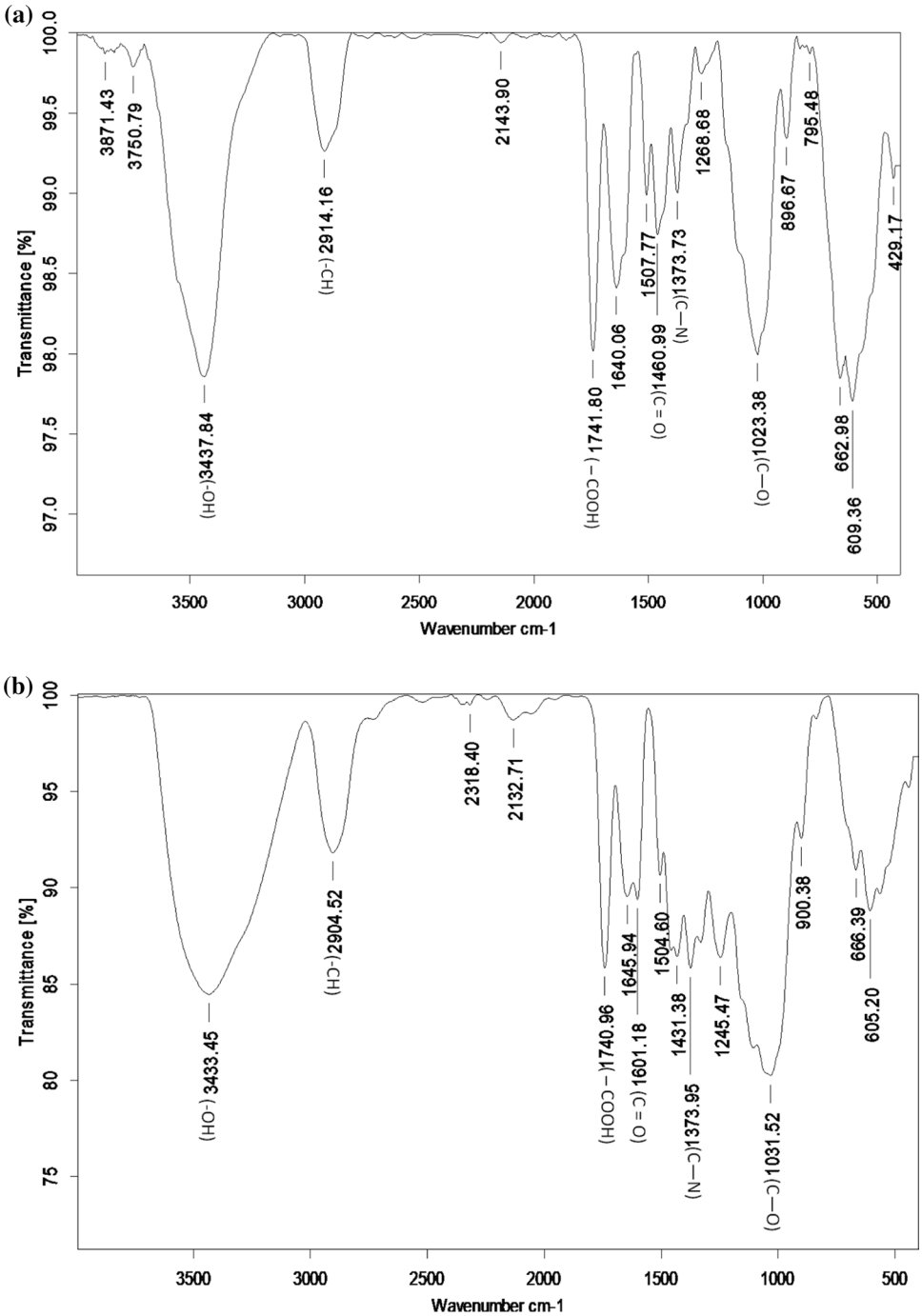

Fig. 3 **a** FTIR spectra of virgin SCTJF before adsorption **b** FTIR spectra of MR-loaded SCTJF after adsorption

stretching vibrations of C=O groups. At 1373.73 cm^{-1}, the C–N stretching band was discovered (Fig. 3a). C–O stretching of alcohols and carboxylic acids was assigned by the band to 1023.38 cm^{-1}. After MR dye adsorption, the symmetrical stretching vibration bands of hydroxyl or amine groups in MR-loaded SCTJF were modified from 3437.84 to 3433.45 cm^{-1}, as shown in Fig. 3b. The stretching band of carboxyl groups was changed from 1741.80 to 1740.96 cm^{-1}. 1640.06 cm^{-1}, 1507.77 cm^{-1}, and 1460.99 cm^{-1} stretching bands were likewise changed to 1645.94 cm^{-1}, 1601.18 cm^{-1}, and 1431.38 cm^{-1} correspondingly. The C–O peak was moved from 1023.38 to 1031.52 cm^{-1}, respectively. Similarly, following adsorption, additional values moved their positions. Thus, it may be inferred that functional groups are the key operators responsible for the binding of MR onto the surface of the SCTJF, which is justified according to the examination of FTIR spectra which shows frequency shifts. Similar results have been reported in earlier research (Dey et al. 2018). Shifts in wavenumbers of hydroxyl, carboxyl and amino groups are the primary reason for adsorption of dye onto SCTJF surface.

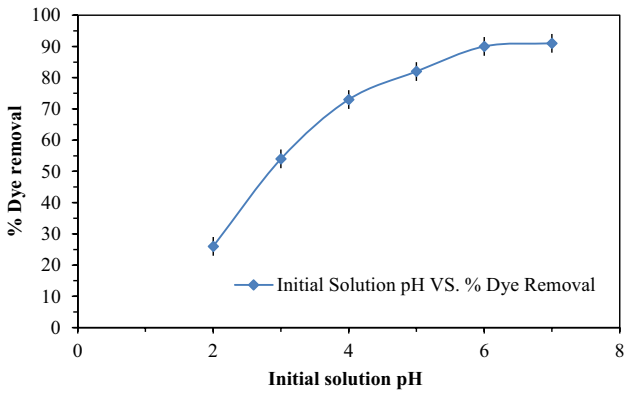

Fig. 4 Percentage removal of MR by SCTJF against pH variation

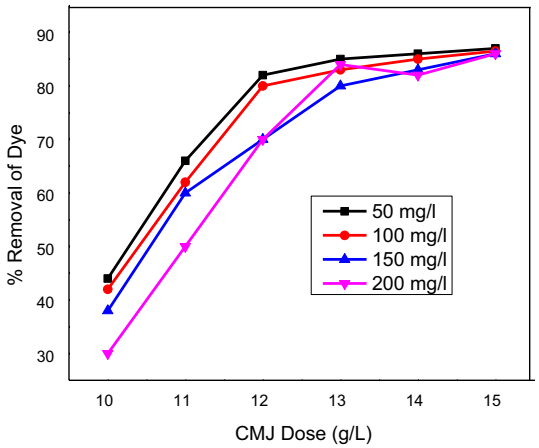

Fig. 5 Percentage removal of dye against SCTJF dose

Analysis of batch study parameters

Effect of pH

In an aqueous solution, pH is a major influencing factor for dye sorption onto adsorbent. In this regard, point of zero charge (pH_{pzc}) plays most vital role in understating how pH of interactive solution dictates the adsorption favourability. The pH at which an adsorbent surface has a net neutral charge is known as the point of zero charge (pH_{pzc}). Study of pH_{pzc} for any adsorbent is of much significance which reveals the potentiality of any adsorbent surface to attract anionic or cationic adsorbates. For example, if a given adsorbent surface has a positive charge at the solution with pH less than pH_{pzc} then that adsorbent surface will uptake adsorbates which are anionic. On the other hand, if that adsorbent surface has a negative charge at the solution with pH greater than pH_{pzc}, then the adsorbent will uptake cationic adsorbate (Webi and Chakravorty 1974; Railsback 2006; Lataye et al. 2006). pH also affects dissociation/ionization and characteristics of sorbent surface and its interaction with adsorbate particles (Freundlich 1906). As a result of the change in surface qualities of both parties (adsorbent–adsorbate), the adsorption process changes. In the present study, it was discovered that as the pH rises, the Q_{max} rises as well. The reason for this is that the functional groups on the adsorbent surface are protonated at low pH causing the absorbent surface to become positively charged, resulting in a low dye ion adsorption due to electrostatic repulsion. And as the pH of the dye solution rises, the adsorption process rises as well, because the adsorbent functional groups will eventually deprotonate, the electrostatic bond between dye cations and negatively charged sites on the adsorbent is increased as a result. The percentage of MR dye removed by SCTJF has been altered by pH, as seen in Fig. 4.

Effect of adsorbent dose

Adsorbent dosage is another significant element to consider when determining the rate of adsorption capacity of the adsorbate onto the adsorbent surface. The dose of SCTJF used to assess the adsorption rate was between 10 and 18 g/L. As the SCTJF dose is increased, there is a noticeable increase in dye adsorption and elimination of dye. This improved dye removal rate with a higher SCTJF dose may be due to a rise in adsorbent surface area, which increases the number of adsorption sites available for adsorption of adsorbates onto the adsorbent (Aksakal and Ucun 2010b). When the SCTJF dose was increased from 10 to 14.8 g/L, the similar result was observed. The absolute adsorption value increases as the SCTJF dose is increased, while the adsorption rate decreases. At a constant dye concentration and a constant volume of solution, the decrease in adsorption rate with a further increase (> 14.8 g/L) in SCTJF dosage may be due to particle interaction such as aggregation, which leads to adsorption site saturation (Chowdhury and Saha 2010b; Mohapatra et al. 2009). Also, it has been observed in our analysis that for any increase in adsorbent dose, keeping the dye concentration constant, absorbance is directly proportional, whereas adsorption rate is inversely proportional. Effect of SCTJF dose on removal of MR dye percentage is depicted using Fig. 5.

Effect of temperature

The adsorption rate is higher at higher temperatures and vice versa, as seen in Fig. 6, revealing endothermic adsorption. The relation between molecules of adsorbate dye and the adsorbent binding site increased as the temperature rises (Chowdhury et al. 2011; Chowdhury and Saha 2010a). This could be because the temperature affects the diffusion (transport pore diffusion, intraparticle diffusion) of the methyl red

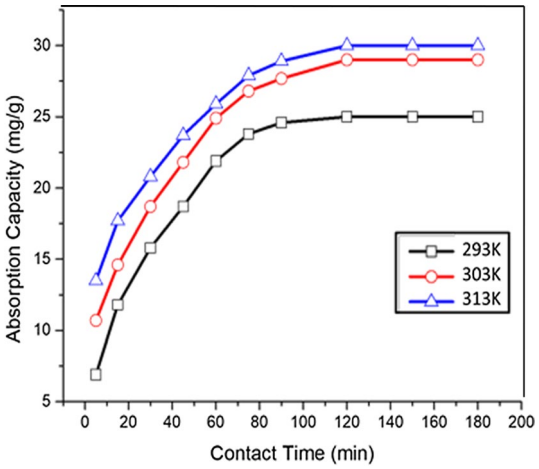

Fig. 6 Effect of Temperature on adsorption capacity

particle, resulting in a larger mass transfer rate from the bulk to the boundary layer surrounding the surface of the jute fibre. It also appears that as the temperature climbed, the pace of the reaction increased as well. The surface becomes activated, resulting in an increase in adsorption capacity. After about 120 min, adsorption process reached equilibrium stage. After this equilibrium period, the amount of dye adsorbed does not show time-dependent change (Dey and Kumar 2017a).

Effect of initial concentration of dye

Figure 7 depicts the effect of initial dye concentration on MR adsorption onto Na_2CO_3-treated jute fibre. The set's experiments were carried out using a sorbent dose of 10 gm/L, a temperature of 303 K, and a pH of 7. The initial concentrations of MR dye in solution considered were 50 mg/L, 100 mg/L, and 150 mg/L. For MR adsorption onto Na_2CO_3-treated jute fibre, the sorption percentage changed from 97.44 to 95.74% when the dye concentration was increased from 50 to 150 mg/L. Mall et al. (2005) reported a similar trend, in which every increase in dye concentration was associated by a decrease in % dye removal.

The saturation of sorption sites on the SCTJF surface can explain this trend. This drop in dye removal percentage could be attributed to the production of a monolayer of dye species on the Jute surface, lowering the likelihood of another layer of dye species forming over the monolayer.

Effect of stirring speed

Adsorption efficacy is strongly determined by the stirring/rotational speed. If the spinning speed (in RPM) is too low, adsorbate and adsorbent particles will tend to settle instead of suspension. If the RPM is too low, both the dye and the jute fibres may sink to the bottom of the conical flask employed for rotating purposes. Both, sorbent and sorbate must remain suspended in order for a persistent dynamic contact between them (adsorbent and adsorbate) and, as a result, for adsorption to occur (Chowdhury and Saha 2010b). Again, if the solution's stirring speed is too high, the chances of adsorption are reduced because a high rotational speed of the solution reduces the capacity of dye particles to settle at the adsorption sites of the adsorbent; instead, a high RPM rate keeps the dye particles floating in the solution, preventing them from settling. The impact of stirring/rotational speed is demonstrated using Fig. 8.

Effect of coexisting anions

Adsorption process can be significantly interfered by the various coexisting anions present in the water body within which adsorption process takes place. For MR sorption using treated jute fibre, batch analysis was carried out to

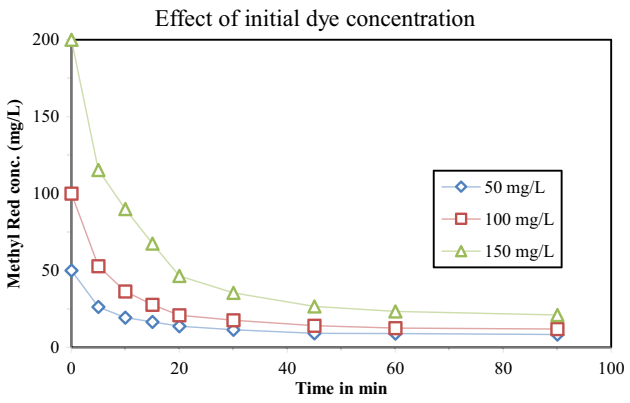

Fig. 7 Influence of initial MR dye concentration onto removal capacity

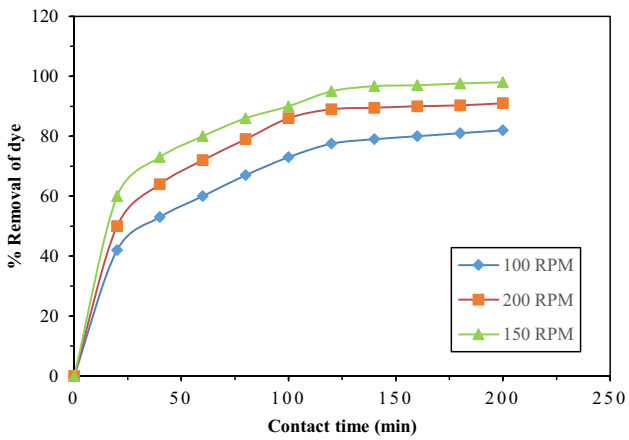

Fig. 8 Percentage removal of dye for different RPM

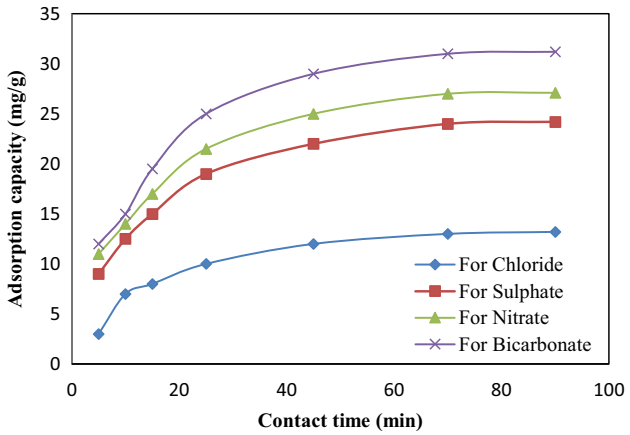

Fig. 9 Plot to show influence of coexisting anions

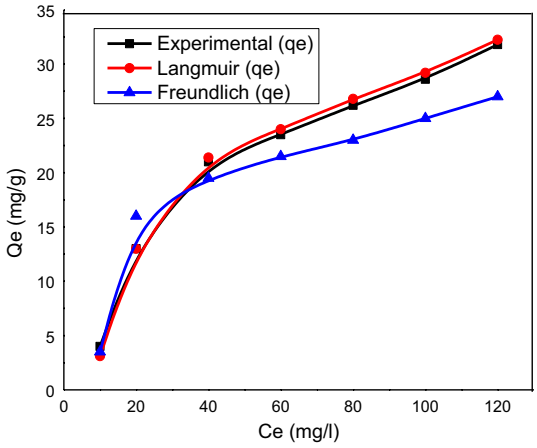

Fig. 10 Langmuir and Freundlich isotherms for MR sorption onto SCTJF at $C_0 = 100$ mg/L, pH = 7.0, RPM = 150, jute dose = 2–10 g/L, $T = 303$ K

find out the influence of coexisting anions, i.e., for bicarbonate, chloride and sulphate and nitrate. Figure 9 reflects the influence of various anions present in the water solution. From the analysis, it was revealed that presence of bicarbonate, nitrate and sulphate substantially effects/hinders the removal process, whereas chloride presence in water do not influence the final outcome of the adsorption process in a considerable manner. Among the influential anions, bicarbonate showed most effectiveness and this can be attributed to the change in the pH of the solution and affinity of this co-ion for adsorbent active site. Hierarchy for the coexisting anion affinity towards the adsorbent was found out as bicarbonate > nitrate > sulphate > chloride which can be observed from the result presented using Fig. 9.

Isotherm study

Establishing the most appropriate correlation for the equilibrium curves is critical for optimising the design of an adsorption system for the removal of adsorbates. The Langmuir, Freundlich, D–R, and R–P isotherm equations were utilised in this study to explain the equilibrium nature of adsorption, and the experimental equilibrium data of MR adsorption onto SCTJF were evaluated using these four equations.

Langmuir and freundlich isotherm models

Below discussed are the two nonlinear adsorption isotherms, namely the Langmuir and Freundlich isotherm studies. Figure 10 shows the plot of the graph of q_e *vs.* C_e, which shows that the mechanism of adsorption better fits the Langmuir Isotherm, implying monolayer adsorption of MR dyes onto the surface of SCTJF. Different isotherm parameters calculated during the analysis are shown using Table 1. Figure 10 shows the adsorption isotherm studies at constant temperature of 303 K.

Dubinin–Radushkevich (D–R) and Redlich–Peterson (R–P) isotherm models

Dubinin–Radushkevich (D–R) has also proposed a model given as:

$$\ln q_e = \ln q_s - \beta\varepsilon^2 \tag{16}$$

where $\varepsilon = RT \ln(1 + \frac{1}{C_e})$.

Table 1 Several isotherm parameters for MR adsorption onto SCTJF

Isotherm model	Constants	Temperature in Kelvin		
		293 K	303 K	313 K
Langmuir	Q_e(mg/g)	27.54	32.11	30.95
	b (L/mg)	8.245	8.915	9.312
	R_L	0.019	0.016	0.025
	R^2	0.895	0.946	0.878
Freundlich	K_F (mg/g)	11.56	11.96	12.87
	N	5.34	6.78	7.13
	R^2	0.866	0.929	0.921
D-R Model	E (kJ/mol)	5.87	5.33	4.98
	Chi square $(\chi)^2$	1.34	1.12	0.87
	P- Value	> 0.90	> 0.95	> 0.95
	R^2	0.995	0.997	0.998
Redlich-Peterson	a_R(L/mg)	1	1	1
	K_R(L/mg)	3.827	3.215	3.977
	B	0.871	0.952	0.981
	R^2	0.998	0.999	0.999

q_e = amount of adsorbate present in the adsorbent at equilibrium (mg/g); q_s = theoretical saturation capacity of isotherm (mg/g); β = Dubinin–Radushkevich isotherm constant (mmol^2 /J.^{2}). To express the mechanism of adsorption with Gaussian energy distribution onto a heterogeneous surface (Mohapatra et al. 2009; Daneshvar et al. 2007), Dubinin–Radushkevich isotherm is generally applied. The idea of mean sorption energy, E, can be obtained by the constant β. This mean sorption energy can be obtained by the relationship given below, and it is defined as the free energy transfer of 1 mol of solute from infinity of the surface of the sorbent

$$E = \left(\frac{1}{2\beta}\right)^{1/2}. \quad (17)$$

The information about the adsorption mechanism such as chemical ion-exchange or physical adsorption can be obtained by the parameter. Chemisorption is supposed to proceed when the magnitude of E is between 8 and 14 kJ/mol, whereas physisorption is supposed to occur for values of E less than 8 kJ/mol, (Zhu et al. 2009).

Redlich–Peterson equation can be expressed as:

$$q_e = \frac{K_R C_e}{1 + a_R C_e^{\beta}} \; or \; \ln\left(K_R \frac{C_e}{q_e} - 1\right) = \ln a_R + \beta \ln C_e. \quad (18)$$

The Redlich–Peterson (R–P) equation incorporates three parameters and can be applied to homogeneous and heterogeneous systems alike. β values between 0 and 1 indicate favourable adsorption. If the adsorption isotherm analysis results reveal that the adsorption is favoured by R–P model, that indicates adsorption occurred in both monolayer and multilayer (Zubair et al. 2022). Langmuir and Freundlich models are, respectively, favourable for monolayer and heterogeneous adsorptions, whereas R–P model can be applied to homogeneous as well as heterogeneous sorption pattern.

It was observed that D–R and R–P models fit better than Langmuir and Freundlich models. Table 1 depicts isotherm parameters for all the four models studied for this research whereas, Figs. 11 and 12 show the plots for D–R and R–P isotherms, respectively.

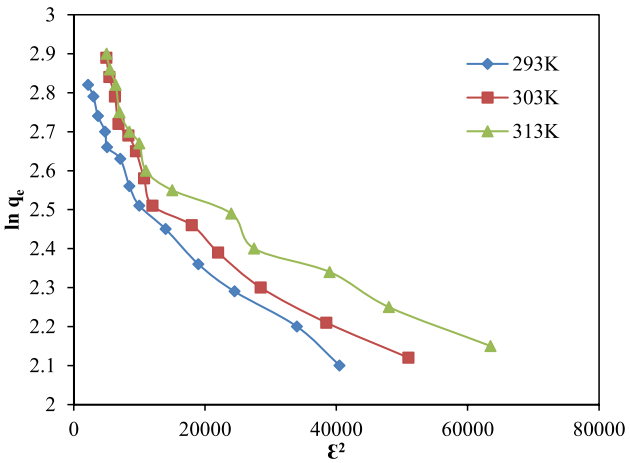

Fig. 11 Plot for D–R isotherm at 293 K, 303 K and 313 K

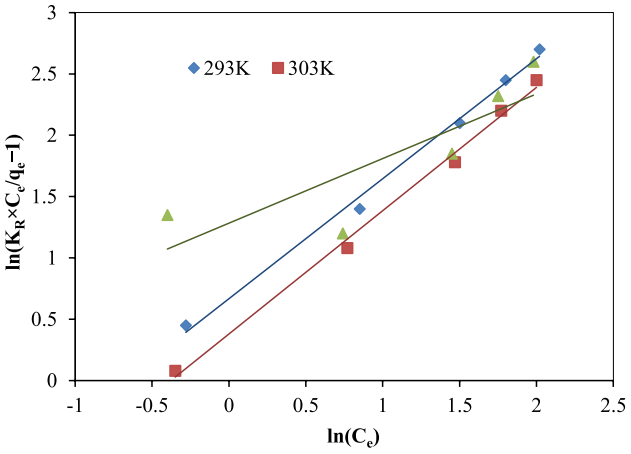

Fig. 12 Redlich–Peterson plot for the removal of fluoride by using bagasse (jute dose = 1 g/L, pH = 7, C_0 = 100 mg/L)

Analysis of rate kinetic models

Two rate kinetic models were studied, namely pseudo-first- and second-order kinetics, and compared with experimental results to determine the rate constants and derive the

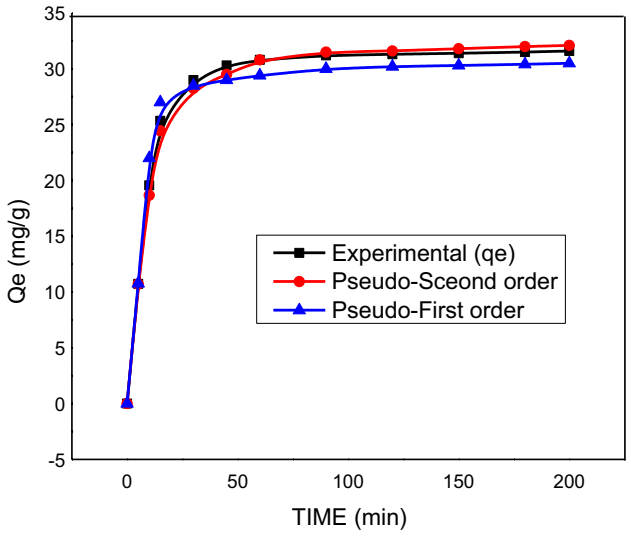

Fig. 13 Pseudo-first- and second-order rate kinetics for MR sorption onto SCTJF at 303 K

adsorption equilibrium capacity at various temperatures. Pseudo-first-order rate constants k_1 and q_e were calculated from the slopes and intercepts of *log* $(q_e - q_t)$ *vs t*. Comparing theoretical and experimental equilibria of pseudo-first-order kinetic model, sorption capacities revealed a significant disparity between this kinetic model and theoretical studies. Same studies showed that experimental data suited more with pseudo-second-order kinetic model. In comparison with the first-order kinetic model for the elimination of MR with SCTJF, Fig. 13 indicates that the pseudo-second-order model matches well with the experimental data.

Elovich model

The Elovich equation is given as (Cheung et al. 2000; Onal 2006):

$$\frac{dq_t}{dt} = \alpha e^{-\beta t} \tag{19}$$

where α = initial rate (mg g^{-1} min^{-1}) and the parameter β (g mg^{-1}) is related to the extent of surface coverage and activation energy for chemisorption.

The linear form of the equation is given as follows:

$$q_t = \frac{1}{\beta}(\alpha\beta) + \frac{1}{\beta}\ln(t). \tag{20}$$

The constants of the Elovich equation are obtained from the plot of *ln(t)* versus q_t as shown in Fig. 14. All the constants of pseudo-first-order, second-order and Elovich model for kinetic studies are listed using Table 2. Among the three models tested pseudo-second-order rate kinetic suited best with the experimental data. Other important studies which can be taken up to show stages of adsorption analysis are IDP model (Zubair et al. 2021).

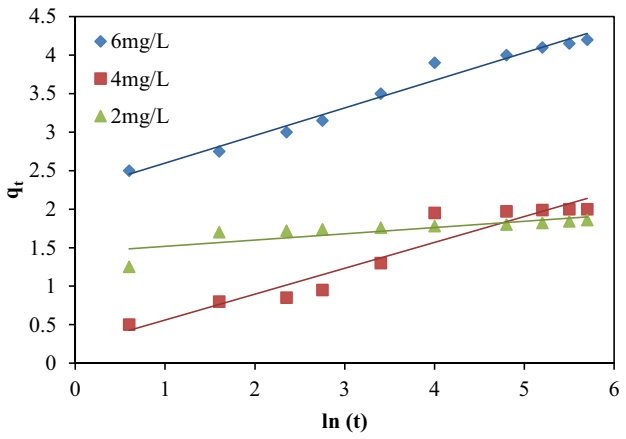

Fig. 14 Elovich plot for MR dye adsorption onto SCTJF, (t = 1 h, pH = 7.0, RPM = 150, Jute dose = 1 g/L)

Table 2 Kinetic constants for studied models

Model constants	Concentration (mg/L)		
	2	4	6
Pseudo first order			
$q_{e,\,exp}$ (mg/g)	1.721	2.673	4.668
$q_{e,\,calc}$ (mg/g)	0.876	1.329	2.425
K_{P1}(min^{-1})	0.0364	0.0384	0.0415
R^2(linear)	0.945	0.946	0.959
Pseudo second order			
$q_{e,\,exp}$ (mg/g)	1.721	2.673	4.668
$q_{e,\,calc}$ (mg/g)	1.314	1.592	2.754
h(mg/g/min)	1.426	1.378	1.845
K_{P2}(min^{-1})	0.0498	0.0436	0.0347
R^2(linear)	0.998	0.999	0.999
Elovich model			
β (g/mg)	10.315	2.991	9.267
α (mg/g/min)	9.432×10^{5}	0.587	2.31×10^{8}
t_0	1.012×10^{-5}	1.172	3.325×10^{-8}
R^2(linear)	0.985	0.978	0.985

Diffusion studies

In pore diffusion, the rate limiting step is determined using the equation proposed by Weber & Morris as:

$$q = K_{id}t^{1/2} + C_i \tag{21}$$

where q is the amount of adsorbate adsorbed in mg/g at time t and K_{id} is the intraparticle rate constant.

This is the form of straight-line $y = mx + c$, where $y = q$, $x = t^{1/2}$, slope $m = K_{id}$ and Y-intercept $= C_i$,

The value of C_i gives an idea of the thickness of boundary layer effect. Larger the intercept, greater the boundary layer effect. If the line passes through the origin, then rate limiting step is only the pore diffusion.

Figure 15 shows the plot for intraparticle diffusion analysis done using Weber and Morris equation. It is revealed

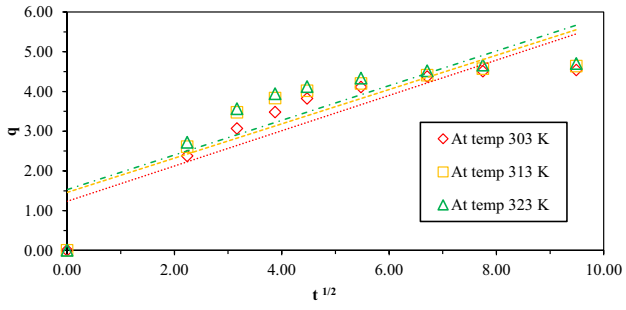

Fig. 15 Plot for q versus $t^{1/2}$ for MR sorption onto SCTJF at temperature 303 K, 313 K and 323 K

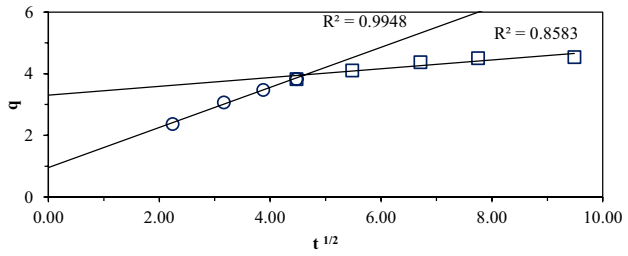

Fig. 16 Plot for q versus $t^{½}$ consisting of multiple straight line for MR sorption onto SCTJF at temperature 303 K

from the figure that the straight line drawn between adsorption capacity and square root of time for the adsorption under investigation do not pass through the origin. For better explanation of intraparticle diffusion, Fig. 16 is illustrated which shows the plot between adsorption capacities for MR dye adsorbed onto SCTJF at time 't' or MR concentration in solid phase at time t and square root of time. It can be seen that the whole plot in Fig. 16 consists of two separate linear lines and none of them intersect at the origin. And as the further enhancement of contact time took place, the magnitude of the intercepts for the linear line also enhanced from the origin, signifying the thickening of the boundary layer; thus, the effect of film diffusion also increased with time. As it was observed from the figures that none of the linear lines pass through the origin, and in fact the intercept kept on increasing with passage of contact time, it can be suggested that both intraparticle diffusion and film diffusion were occurring simultaneously for the sorption of MR dye and onto SCTJF.

Activation energy and thermodynamic parameters

The method's activation energy E_a was calculated using the Arrhenius equation (Eq. 12, Sect. 2.4) and the Arrhenius plot of MR adsorption on SCTJF. It was carried out to determine the type of adsorption occurring in the process, and it thus plays an important role in establishing whether the adsorption is physical or chemical. Physical adsorption is indicated by a low E_a value (< 40 kJ/mol), while chemical adsorption is indicated by a higher E_a value (≥ 40 kJ/mol) (Dey and Dey 2021a). In the present analysis, adsorption rate was better suited to second-order rate constant kinetics in this investigation; hence, the plot was made with ln K (K = pseudo-second-order rate constant) values in the Y axis and $1/T$ (time inverse in Kelvin) in the X axis. E_a was calculated using the linear graph's slope, which equals 43.45 kJ/mol. We can conclude from this that the subsequent process is mostly controlled by chemisorption (Dey and Dey 2021a). The Arrhenius plot for determining E_a is shown in Fig. 17.

One of the thermodynamics parameters, change in Gibb's free energy ($\Delta G°$), was estimated using the values

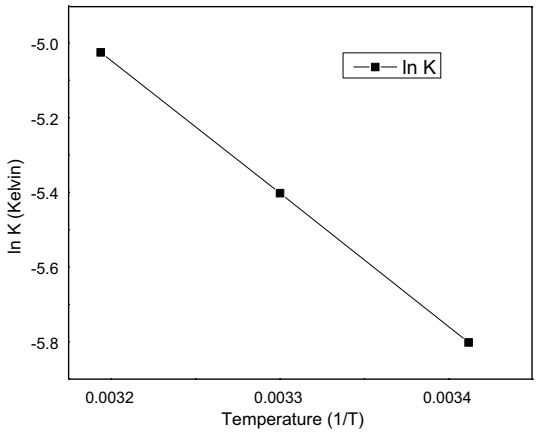

Fig. 17 Arrhenius plot for MR dye sorption onto SCTJF

of the equilibrium rate constant (K_{ad}), and the intercepts of the graph of $\Delta G°$ vs. T (time) were used to determine the other two parameters, entropy ($\Delta S°$) and enthalpy ($\Delta H°$). The parameters were determined using Eqs. 13, 14, and 15 (Sect. 2.4) in addition to the plot. $\Delta G°$ was determined to be -1.84, -5.23, and -9.12 kJ/mol for temperature values of 293 K, 303 K, and 313 K, respectively. With an increase in temperature, the value of change in Gibb's free energy decreased, indicating that the adsorption process was suitable at moderate to high temperature. With a rise in temperature, the adsorption capacity increased, implying an enhancement in the kinetic energy of sorbent particles. $\Delta S°$ value being positive (0.162 kJ/mol K) indicates an increase in randomness at the solid/solution interface, which is entropy driven. The presence of a positive $\Delta H°$ (12.35 kJ/mol) indicates that the process is endothermic (Saeed et al. 2010; Yagub et al. 2012; Vadiveloo et al. 2009). The value of $\Delta H°$ determines the nature of the adsorption process;

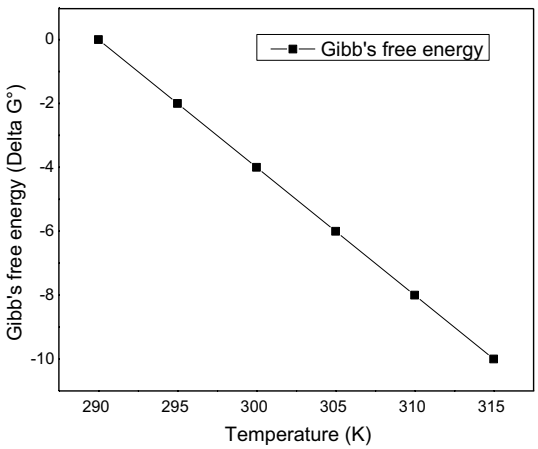

Fig. 18 ΔG° (change in Gibb's free energy) versus T (temperature) for MR sorption onto SCTJF

Table 3 Parameters from thermodynamics for MR sorption onto SCTJF

Parameters	Temperature in Kelvin		
	293 K	303 K	313 K
ΔG° (KJ/mol)	− 1.84	-5.23	− 9.12
ΔS° (KJ/mol K)	–	0.162	–
ΔH° (KJ/mol)	–	12.35	–

in general, physical adsorption happens when the value is between 8 and 25 kJ/mol, while chemical adsorption occurs when the value is between 80 and 200 kJ/mol (Dey and Dey 2021a). The nature of adsorption is proven to be physical in this investigation by measuring the ΔH° value, which validates the study of activation energy. Figure 18 depicts the plot of ΔG° *vs* T. The different thermodynamic parameters are shown in Table 3.

Cost analysis

Cost analysis was done for the amount of SCTJF used in the whole experimentation, and the same has been compared with that of activated carbon. Studies revealed that use of SCTJF incurred around 7.11 Indian rupee for our research, whereas if the same amount of commercially available activated carbon would have been used, then that would have incurred a cost of 181.6 Indian rupee. The same has been depicted using Table 4.

Adsorption optimization using RSM

Batch-wise analyses were used to estimate the maximum adsorption capacity (Q_{max}) as a function of pH, temperature (K), SCTJF dose (g/L), and rotational speed (in RPM). This was achieved by altering one of the process parameters while leaving the others constant, several Q_{max} values were assessed in a series. Similarly, using response surface approach, Q_{max} values were found 30 times by executing 30 different sets of process parameter combinations, which were then used to find the most desirable state. RSM is a statistical and mathematical technique that is used to optimise and model response characteristics, which include quantitative independent elements. As shown in Eq. 3 in the introduction section, a regression model, also known as a polynomial quadratic model of order two, explains the system quality characteristic. The coefficient of the regression model is calculated using Eq. 3, using modelling tool "Design Expert 11.0."

The current study's experimental design was primarily based on the face-cantered central composite second-order design (CCD) method. The CCD full factorial design, which includes eight-star points and six centre points (coded level 0), corresponds to an α (alpha) value of 1 when all factors are combined at two levels (high, + 1, and low, −1). The 'face-centred CCD' is made up of 30 trials with four process variables. Table 5 shows the appropriate range of process parameters, as well as their coded and real values. The coded version of the experimental design layout used in this study is shown in Table 6.

The model fit summary stated that the second-order quadratic model had a lot of relevance when compared to the statistical analysis of Q_{max}. The findings of the quadratic model's study are shown in Table 7 using ANOVA. The model F value reflects the model's importance. The chance of F value for the model's term being more than 0.95 (i.e., = 0.05, or 95% confidence) indicates that the model developed should be statistically significant and mandatory, as it implies that the model terms affect performance attributes (Kansal et al. 2007). When the value of multiple coefficients of regression R^2 is close to unity, the response models suit the real data better. The gap between real and anticipated values narrows considerably. Figure 19, which depicts a graph between the actual and expected response levels, demonstrates the

Table 5 Experimental operating parameters with range of levels

Parameters	Factors	Levels		
		− 1	0	+ 1
pH	A	3	7	11
Temperature, (^{0} K)	B	293	303	313
SCTJF dose, (g/l)	C	10	14	18
Rotational speed, (RPM)	D	100	150	200

Table 4 Cost comparison of SCTJF with activated carbon

Material used	Unit cost (Rs.)	Quantity used	Net cost (Rs.)
Jute fibre	56/Kg	15 g	0.84
Na_2CO_3 (sodium carbonate)	325/Kg	5 g	1.625
Drying cost	5/kWh	0.80 kWh for 6 h	4.0
Other miscellaneous expenses (10% of materials and drying costs)	–	–	0.64
Total cost			7.11
Commercially available activated carbon	12,107.2/Kg	15 g	181.6

Table 6 Design layout and experimental results

Exp. no	Factor1 A: pH	Factor 2B: temp	Factor 3C: SCTJF dose	Factor 4D: RPM	Response Q_{max} (mg/g)
1	3	313	10	200	10.21
2	3	293	10	100	11.42
3	11	293	18	200	15.67
4	3	313	10	100	5.19
5	11	313	18	100	10.43
6	3	313	18	200	12.69
7	3	293	10	200	11.76
8	11	293	10	200	11.28
9	7	303	14	150	31.91
10	11	313	10	200	11.19
11	11	313	10	100	11.01
12	7	303	14	150	30.98
13	7	303	14	150	31.56
14	3	293	18	100	12.64
15	3	293	18	200	16.34
16	11	313	18	200	13.41
17	11	293	10	100	11.29
18	11	293	18	100	13.38
19	3	313	18	100	11.31
20	7	303	14	150	30.59
21	7	303	14	150	32.11
22	7	303	14	150	31.89
23	7	303	14	100	28.48
24	3	303	14	150	24.91
25	7	303	10	150	27.21
26	7	293	14	150	28.29
27	7	313	14	150	27.28
28	7	303	14	200	26.19
29	7	303	18	150	29.56
30	11	303	14	150	27.87

degree of proximity (Q_{max}). Most of the data points are near to a straight line, indicating that the errors were regularly distributed. In this investigation, the value of appropriate precision (AP) for the proposed regression model, as defined by ANOVA, was greater than 3. The expected value span at the design point is compared to the mean prediction error with the help of AP to evaluate if the model discrimination is sufficient. According to the created model, the coefficients of determination (R^2) have a greater value and the precision is appropriate. The findings of the presented analysis were $R^2 = 0.95$ and AP = 14.68 for Q_{max}. As a result, the built quadratic mathematical model has a major impact on fitting and predicting observational results, but the lack-of-fit test has no bearing (refer Table 7). In order to localise the fitted quadratic response surface models, the backward elimination technique was utilised to remove insignificant/insignificant components. The lack-of-fit test is determined to be unimportant when the insignificant quadratic model terms are removed. Multiple response surface graphs were created for the same purpose of analysing Q_{max} under various operating circumstances, as shown in Fig. 20. Figures 20a, 22b, c show the approximated response surface plot for Q_{max} in relation to solution process factors such as pH, SCTJF dose, temperature, and rotational speed (in RPM).

Multi response optimization based on desirability criteria

Table 8 shows the goals and ranges of operating process variables such as SCTJF dosage, pH, Temperature and rotational speed (RPM), as well as response parameter Q_{max}. The RSM approach purpose is to find a set of optimal operating conditions that will help achieve the primary objective. Because the value is solely dependent on how closely the upper and lower limits are determined to be placed relative to the genuine optimum, the 1.0 desirability value is not the absolute requirement.

Statistical Design Expert software 11.0 is used to find an optimal solution consisting of 30 sets for the specified design space restrictions for Q_{max}. The collection of parametric circumstances with the highest desirability value is picked as the best processing condition for the intended performance characteristics (Vankar 2000; Zhou et al. 2015). Table 9 shows the best parametric condition with the highest desirability function. Once the ideal set of input parameters has been found, the ultimate measure is the identification and verification of the augmentation of response characteristics by employing the optimal level of processing parameters. A confirmation test was done at the optimum setting of process parameter for rotating speed (RPM), pH, SCTJF dose, and temperature to examine and compare with the ideal value of response characteristics. The error percentage obtained for experimental validation of the created response models with the best process parameter setting at the time of experimentation is shown in Table 10 revealing minimal percentage error of 1.2.

Figures 21 and 22 show the desirability function for performance attributes using a graph of a ramp function and a bar graph, respectively (Taweel 2009). The parameter settings or response prediction for each performance feature are shown by each dot on the ramp. The level of desirability of the reaction is revealed by the dot's elevation. A linear ramp function is generated between the objective and the high value, or between the target and the high value, with the value of each weight component equal to one (Rahman et al. 2018). The function of overall desirability of quality behaviours is determined using

Table 7 The ANOVA results for Q_{max}

Source	Sum of squares	df	Mean square	*F*-value	*p*-value	Remark
Model	2241.69	14	160.12	29.34	< 0.0001	significant
A-pH	4.56	1	4.56	0.8356	0.3751	–
B-Temperature	22.38	1	22.38	4.10	0.0610	–
C-SCTJF dose	40.11	1	40.11	7.35	0.0161	–
D-RPM	15.29	1	15.29	2.80	0.1149	–
AB	3.22	1	3.22	0.5904	0.4542	–
AC	2.46	1	2.46	0.4517	0.5118	–
AD	1.56	1	1.56	0.2863	0.6004	–
BC	0.2601	1	0.2601	0.0477	0.8301	–
BD	0.6561	1	0.6561	0.1202	0.7336	–
CD	1.45	1	1.45	0.2661	0.6135	–
A^2	132.43	1	132.43	24.27	0.0002	–
B^2	13.64	1	13.64	2.50	0.1348	–
C^2	44.71	1	44.71	8.19	0.0119	–
D^2	84.31	1	84.31	15.45	0.0013	–
Residual	81.86	15	5.46	–	–	–
Lack of Fit	81.25	10	8.12	66.67	0.114	Insignificant
Pure Error	0.6093	5	0.1219	–	–	–
Cor Total	2323.55	29	–	–	–	–

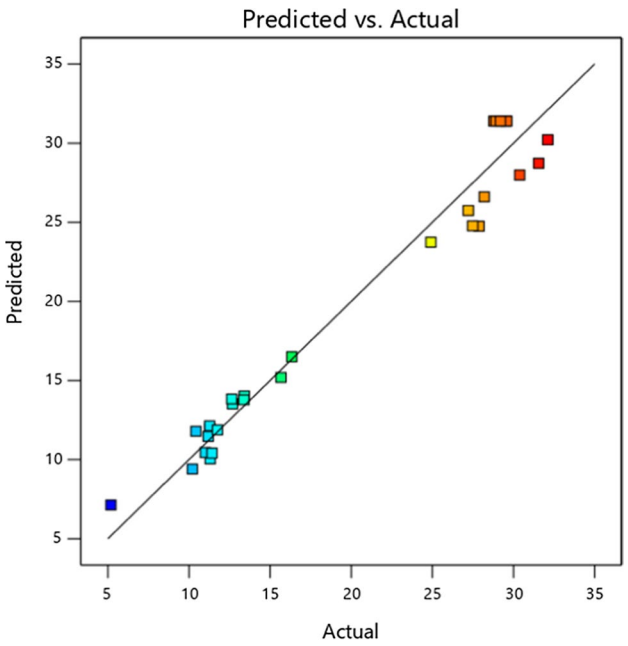

Fig. 19 Predicted vs. actual plot for Q_{max}

a bar graph. The value of desirability fluctuates from 0 to 1 depending on how close the response is to the goal. The bar graph depicts the appropriateness of each process variable to the design criterion, with values around one indicating good suitability.

With process parameters in range and maximum response characteristics, a Q_{max} 3D desirability graph was created. The distribution of the desirability function for the expected response of Q_{max} inconsonance with temperature and pH is depicted in Fig. 23. As can be seen, the value of overall desirability decreases as the pulse current and pulse on time regions increase. The optimal desirability zone was found around the top of the plot, where the total desirability value was larger than 0.98 and gradually declined as the plot moved to the right and backwards. As a result, the revealed desirability value of 0.98 depicts the response's proximity to the target (Dey and Pandey 2018b; Dey et al. 2017, 2022; Niraj et al. 2018; Su et al. 2013).

Adsorption mechanism

Understanding the mechanism of adsorption is one of the most fascinating aspects of any adsorption investigation. To do so, two things are of prime importance: (1) the adsorbate structure and (2) the functional groups present in an adsorbent that are responsible for adsorption. According to the current study on methyl red (MR) adsorption, the MR dye molecule comprises amino groups that establish hydrogen bonds with the exposed hydroxyl groups in SCTJF (Koch et al. 2002; Lagergren 1898; Langmuir 1916). Treatment of jute fibre with Na_2CO_3 affects the surface morphology, lowers the silica concentration, and increases the crystallinity of the cellulose fraction, according to the results of SEM

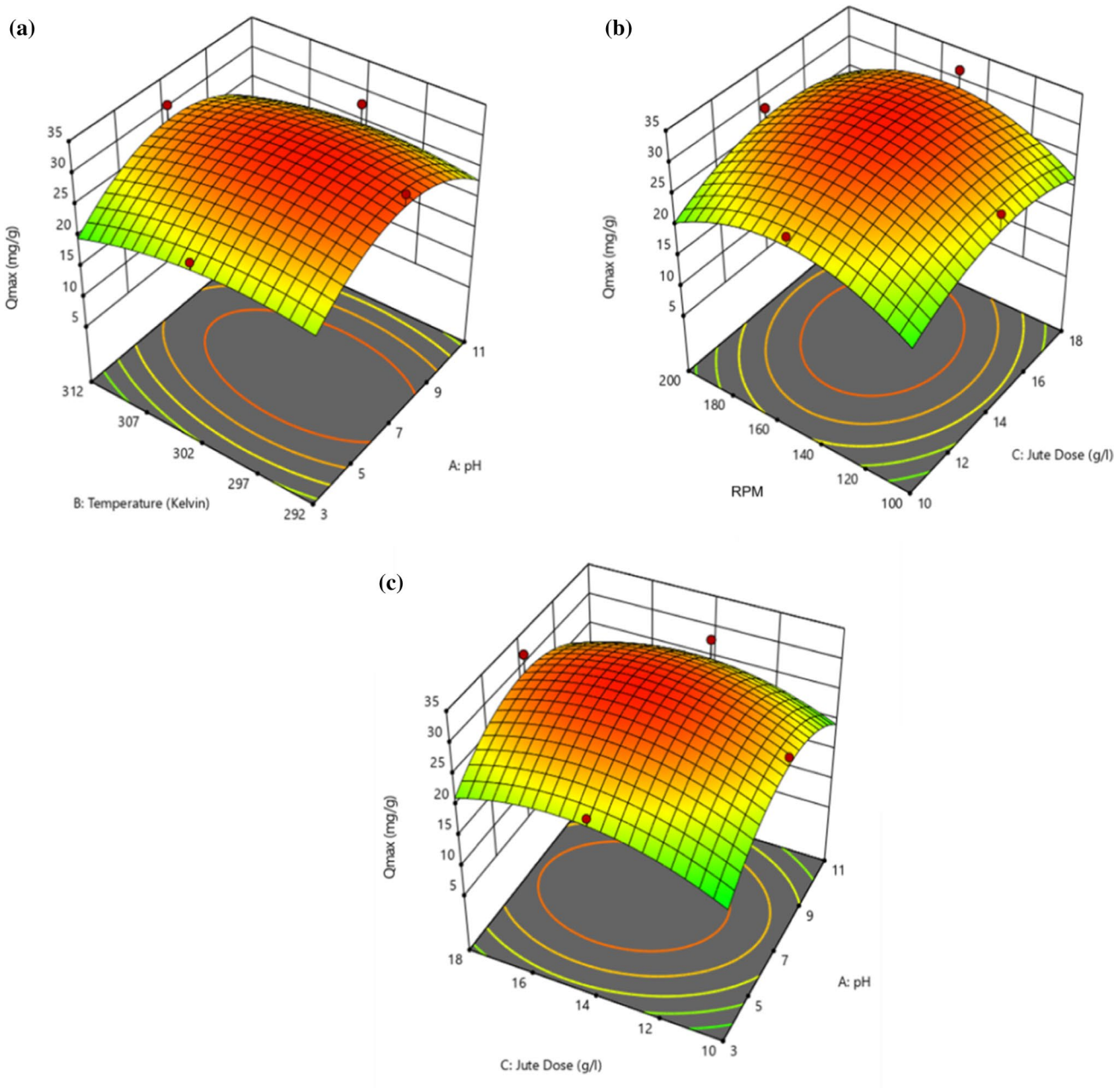

Fig. 20 Q_{max} response surface plot, **a** temperature vs. pH, **b** RPM vs. SCTJF dose; and **c** SCTJF dose vs. pH

Table 8 Desirability responses based on range of input parameters

Name	Goal	Lower limit	Upper limit	Lower weight	Upper weight	Importance
A:pH	Is in range	3	11	1	1	3
B:Temperature	In range	293	313	1	1	3
C:SCTJF dose	Is in range	10	18	1	1	3
D:RPM	Is in range	100	200	1	1	3
Q_{max}	Maximize	5.19	32.11	1	1	3

Table 9 Optimum values depending upon input operating parameters

Parameter	Goal	Optimum value
pH	in range	7.1
Temperature, (K)	in range	299.56
SCTJF dose, (g/l)	in range	14.7
Rotational speed, (RPM)	in range	154

Table 10 Q_{max} responses, predicted and experimental values

Responses	Goal	Predicted value	experimental value	Error (%)
Q_{max} (mg/g)	Maximize	31.7	32.11	1.2

and FTIR tests. The same has been extensively explored in part 2 of this article. Because dye ions are better linked to the changed and appropriate adsorbent molecular structure, this change in surface features of treated jute fibre will likely favour chemical reaction between the hydroxyl exposed adsorbent and dye ions, as well as mechanical bonding.

As described in Sect. 3, all of the experiments had a very rapid rate of adsorption for the first 20–25 min, which then gradually slowed until the equilibrium time was reached at 120 min, implying that there was mostly intraparticle diffusion assisted by film diffusion. Sorption capacity was greatest at pH 7.0, and the SCTJF dose and RPM were important factors in determining it. The following adsorption mechanism can be inferred based on the findings:

- MR dye transfer from the solution to the surface of the Jute fibre.
- Diffusion of dye particles from aqueous solution to the adsorbent surface via the boundary layer.
- The formation of a hydrogen bond between the dye's amino groups and the exposed hydroxyl group in the jute fibres is thought to be the cause of dye molecule adsorption on the surface of jute fibres. Figure 24 depicts the general mass transfer process in adsorption. Figure 25 depicts the adsorption method employing functional groups

Methyl red desorption study

To be an applicable adsorbent, it should be cost-effective, and for that it is critical that the MR dye adsorbed should be readily desorbed for the reusability of the used media. MR dye desorption from used sorbents was experimented at various pH values (2–10). An initial concentration of 4 mg/L, temperature of 313 K, an

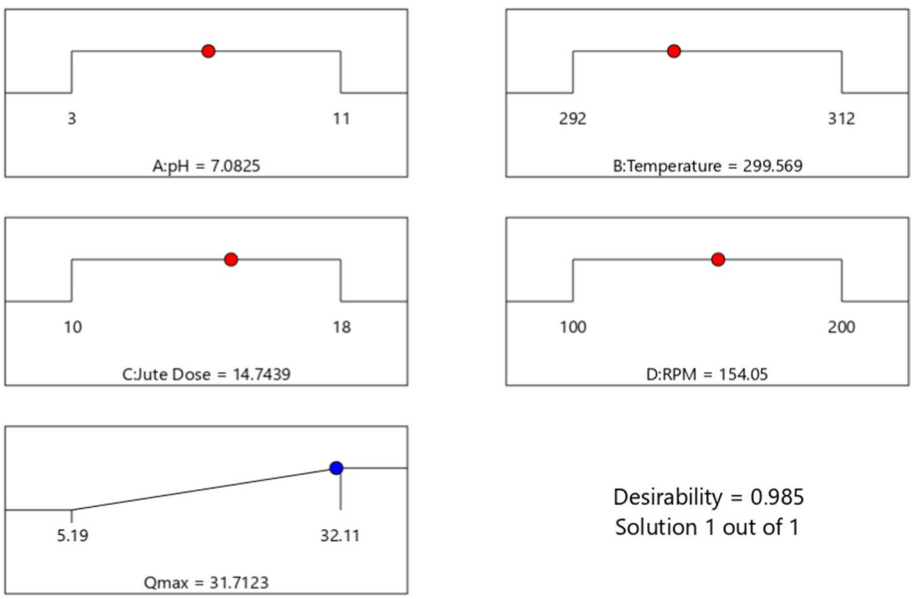

Fig. 21 Ramp function plot of desirability for Q_{max}

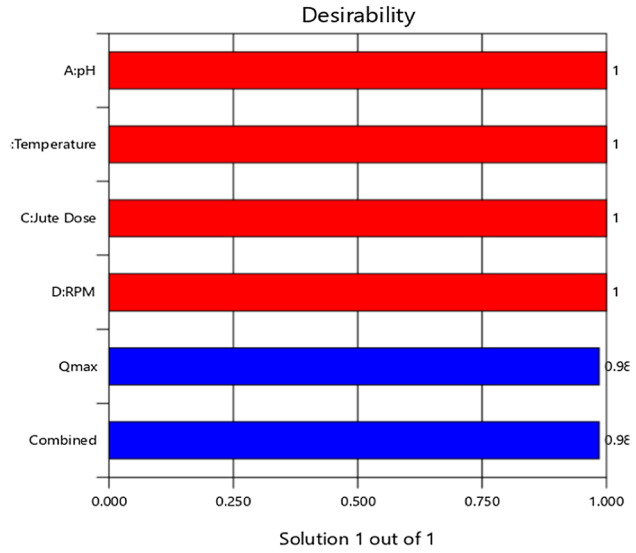

Fig. 22 Bar graph of desirability Q_{max}

optimum dose of 1 g/L and time of 1 h were used for desorption study. Analysis yielded a non-encouraging result of 5–6% desorption. Around 85% of world's jute production is concentrated in the Ganges Delta (Bangladesh, India) and parts of China (Dey and Kumar 2017a). From the experimental result, it may thus be concluded that jute fibre desorption efficiency was low, and a significant amount of MR dye could not be desorbed. Based on the sample desorption analysis, further desorption and regeneration of used jute fibre is not advised. So, to recuperate the energy value, the used jute fibre can simply be filtered out of the mixture, dewatered, sun-dried, and then can be used as a filler material in furniture making products like plywood, can be burnt as fuel into a furnace or boiler. Finally, it is recommended that instead of regenerating the adsorbents, it is more cost-effective to use them in an exhaustive manner or dispose them.

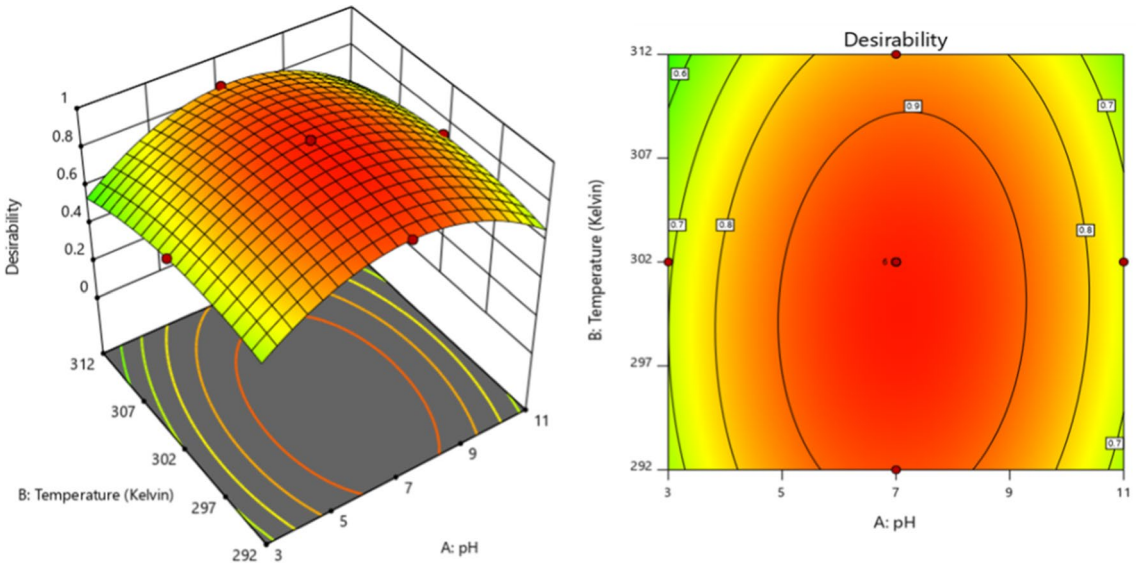

Fig. 23 3D Surface plot of desirability of Q_{max} for temperature and pH

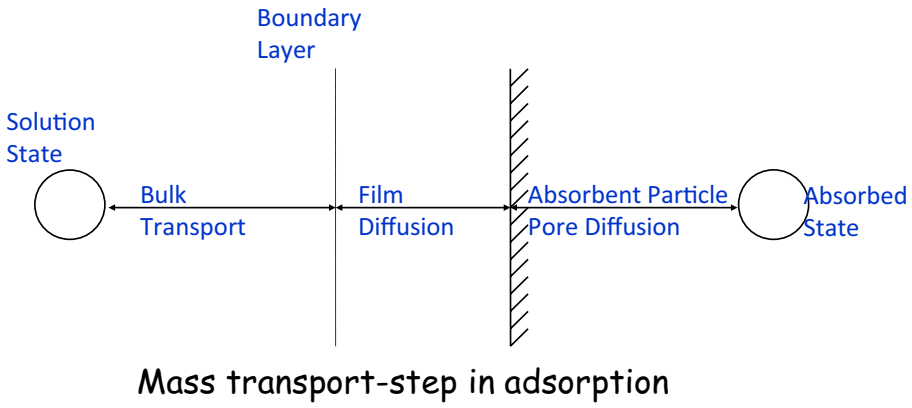

Fig. 24 Boundary layer diffusion phenomena in adsorption

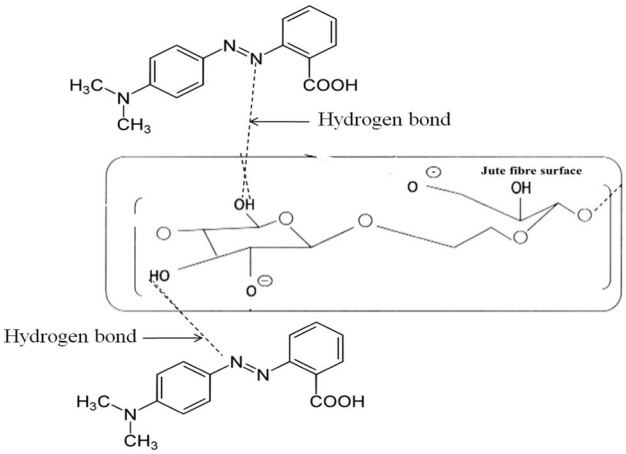

Fig. 25 Mechanism for MR sorption onto SCTJF

Comparative results for MR dye removal using various non carbon adsorbents

Comparative analysis results for the removal of MR dye using various non-carbon-based adsorbents are shown using Table 11. Adsorbents used for analysis results shown are all modified from various agricultural waste or other type of modified adsorbents.

Conclusions

Analysis was done to check the feasibility and efficacy for the removal of an anionic azo dye methyl red (MR) using chemically (Na_2CO_3) modified jute fibre with the aid of adsorption technology using composite design face-centred central (CCD) RSM. Using 30 experimental trials with three repetitions in each of the process parameters at three different levels, the effect of input process/operating parameters such as SCTJF dose, pH, Temperature, and stirring speed was successfully investigated for designing the output of maximum adsorption capacity. The findings of the modelling show that within the studied range of operating parameters, moderate to high SCTJF dosage, moderate RPM, moderate to high temperature and neutral pH are critical for optimal adsorption capacity. The computed R^2 value of 0.98 for Q_{max} justifies the same, demonstrating the model's adequacy. Two consequential factors that influenced the outcome of Q_{max} were the SCTJF dosage and pH. In the respective parts of this article, the influence of each process parameters and their justifications are examined. For maximising the Q_{max}, the ideal parameter settings were found to be as rotational speed 154 RPM, temperature 299.56 K, SCTJF dosage 14.74 gm/L, and pH 7.08. The methodology's precision is confirmed by the satisfactory error percentage of 1.2 between the anticipated and actual values for Q_{max}. Desorption study showed that regeneration of used adsorbent will not be cost-effective.

Table 11 MR Dye removal using various non-carbon-based adsorbent

Sl. no	Type of adsorbent	Maximum adsorption capacity (Q_{max})	References
1	Modified coconut husk	71 mg/g	Aziz et al. 2016)
2	Water hyacinth (*eichornia crassipes*) biomass	8.85×10^{-2} mol/g	Tarawou et al. 2007)
3	White potato peel powder	30.48 mg/g	Enenebeaku et al. 2017)
4	Natural and purified organic matter rich clay	397 mg/g	Romdhane et al. 2020)
5	Banana pseudostem fibres	96.39%	RSM, T. D. M. K. P. S. 2014)
6	Bentonite type clay from mostaganem region (MBC)	2 mg/g	Boudouara et al. 2014)
7	Shell of the cocoa pod	6.39 mg/g – 13.88 mg/g	Lafi et al. 2022)
8	Eggshell powder (ESP)	1.66 mg/g	Rajoriya et al. 2021)
9	Na_2CO_3 modified jute fibre	32.11 mg/g	This study

Funding The authors received no specific funding for this work.

Declarations

Conflict of interest On behalf of all authors, the corresponding author states that there is no conflict of interest.

References

Aksakal O, Ucun H (2010a) Equilibrium, kinetic and thermodynamic studies of the biosorption of textile dye (Reactive Red 195) onto Pinussylvestris L. J Hazar Mater 181:666

Aksakal O, Ucun H (2010b) Equilibrium, kinetic and thermodynamic studies of the biosorption of textile dye (Reactive Red 195) onto Pinus sylvestris L. J Hazard Mater 181:666–672

Aziz EA, Razak AA, Sulaiman S, Halim HA, Islam MS, Zainodin NA, Omar WW (2016) The performance of coconut husk and shell for the removal of methyl red from aqueous solution: adsorption equilibrium and kinetic study. J Eng Appl Sci 11(11):2500–2507

Boudouara K, Ghelamallah M, Khemliche HN (2014) Adsorption of methyl red from aqueous solutions by Algerian bentonite clay. In *2nd international congress on energy efficiency and energy related materials (ENEFM2014)*, Springer. Cham, pp. 203–209.

Chen Y, Zhang D (2014) Adsorption kinetics, isotherm and thermodynamics studies of flavones from vacciniumbracteatumthunb leaves on NKA-2 resin. Chem Eng J 254:579

Cheung CW, Porter JF, Mckay G (2000) Sorption kinetics for the removal of copper and zinc from effluents using bone char. Sep Purif Technol 19(1–2):55–64

Chiang KT (2008) Modelling and analysis of the effects of machining parameters on the performance characteristics in EDM process of Al_2O_3 + TiC mixed ceramic. Int J Adv Manuf Technol 37:523

Cho H, Joh KD (2007) Photocatalytic degradation of azo dye (Reactive Red 120) in TiO_2/UV system: Optimization and modelling using a response surface methodology (RSM) based on the central composite design. Dye Pigm 75:533

Chong MN, Jin B, Chow CWK, Saint CP (2009) A new approach to optimize an annular slurry photoreactor system for the degradation of Congo red: statistical analysis and modelling. Chem Eng J 152:158

Chowdhury S, Saha P (2010a) Sea shell powder as a new adsorbent to remove basic green 4 (malachite green) from aqueous solutions: equilibrium, kinetic and thermodynamic studies. Chem Eng J 164:168

Chowdhury S, Mishra R, Saha P, Kuskwaha P (2011) Adsorption thermodynamics, kinetics and isosteric heat of adsorption of malachite green onto chemically modified rice husk. Desalination 265:159

Crini G, Peindy HN, Gimbert F, Robert C (2007) Removal of C.I. Basic Green 4 (Malachite Green) from aqueous solutions by adsorption using cyclodextrin-based adsorbent: kinetic and equilibrium studies. Separ Purif Technol 53:97

Daneshvar N, Khataee AR, Pourhassan M (2007) Biological decolorization of dye solution containing Malachite Green by CRoalgae Cosmarium. Biores Technol 98(6):1176–1182

Dey AK, Dey A (2021a) Selection of optimal processing condition during removal of Reactive Red 195 by NaOH treated jute fibre using adsorption. Groundw Sustain Dev 12:100522

Dey AK, Kumar U (2017a) Adsorption of anionic azo dye Congo Red from aqueous solution onto NaOH-modified jute fibre. Desalin Water Treat 92:301–308

Dey AK, Kumar U (2017b) Adsorption of reactive red 195 from polluted water upon Na_2CO_3 modified jute fibre. Int J Eng Technol 9(3S):53–58

Dey A, Pandey KM (2018a) Wire electrical discharge machining characteristics of AA6061/cenosphere as-cast aluminum matrix composites. Mater Manuf Proc 33(12):1346

Dey A, Pandey KM (2018b) Selection of optimal processing condition during WEDM of compocasted AA6061/cenosphere AMCs based on grey-based hybrid approach. Mater Manuf Proc 33(14):1549

Dey A, Debnath M, Pandey KM (2017) Analysis of effect of machining parameters during electrical discharge machining using Taguchi-based multi-objective PSO. Int J Comp Intel App 16(02):1750010

Dey AK, Kumar U, Dey A (2018) Use of response surface methodology for the optimization of process parameters for the removal of congo red by NaOH treated jute fibre. Desalin Water Treat 115:300–314

Dey AK, Dey A, Goswami R (2022) Fixed-bed column analysis for adsorption of Acid scarlet 3R dye from aqueous solution onto chemically modified betel nut husk fibre. Desalin Water Treat 252:381–390

AK Dey, A Dey (2021b) Selection of optimal processing condition during removal of methylene blue dye using treated betel nut fibre implementing desirability based rsm approach. Response surface methodology in engineering science. ISBN: 978–1–83968–918–5.

Enenebeaku CK, Okorocha NJ, Uchechi EE, Ukaga IC (2017) Adsorption and equilibrium studies on the removal of methyl red from aqueous solution using white potato peel powder. Int Let Chem Phys Astro 72:52

Freundlich HMF (1906) Over the adsorption in solution. J Phys Chem 57:385

Ganguly PK, Chanda S (1994) Dyeing of jute: effect of progressive removal of hemicellulose and lignin. Ind J Fibre Tex Res 19:38

Gupta VK, Pathania D, Sharma S, Agarwal S, Singh P (2013) Remediation and recovery of methyl orange from aqueous solution onto acrylic acid grafted ficus carica fiber: isotherms, kinetics and thermodynamics. J Mol Liq 177:325

Ho YS, McKay G (1999) Pseudo-second-order model for sorption processes. Proc Biochem 34:451

Ibrahim S, Fatimah I, Ang HM, Wang S (2010) Adsorption of anionic dyes in aqueous solution using chemically modified barley straw. Water Sci Technol 62:1177

Kansal HK, Singh S, Kumar P (2007) Technology and research developments in powder mixed electric discharge machining (PMEDM). J Mater Process Technol 184:32

Kapdan IK, Ozturk R (2005) Effect of operating parameters on color and COD removal performance of SBR: sludge age and initial dyestuff concentration. J Hazard Mater B123:217

Koch M, Yediler A, Lienert D, Insel G, Kettrup A (2002) Ozonation of hydrolyzed azo dye reactive yellow 84 (CI). Chemosphere 46:109

Kumar S, Basu A, Dutta S (2012) Application of response surface methodology for methylene blue dye removal from aqueous solution using low cost adsorbent. Chem Eng J 289:181–182

Lafi R, Abdellaoui L, Montasser I, Mabrouk W, Hafiane A (2022) The effect of head group of surfactant on the adsorption

of methyl red onto modified coffee residues. J Mol Struct 1249:131527
Lagergren S (1898) About the theory of so-called adsorption of soluble substances. Kun Sve Veten Hand 24:1
Langmuir I (1916) The constitution and fundamental properties of solids and liquids. J of Amer Chem Soc 38:2221
Lataye DH, Mishra IM, Mall ID (2006) Removal of pyridine from aqueous solution by adsorption on bagasse fly ash. Ind Eng Chem Res 45(11):934–3943
Lataye DH, Mishra IM, Mall ID (2008) Multicomponent sorptive removal of toxics-pyridine, 2-picoline and 4-picoline from aqueous solution by bagasse fly ash: optimization of process parameters. Ind Eng Chem Res 47(15):5629–5635
Liang S, Guo X, Feng N, Tian Q (2010) Isotherms, kinetics and thermodynamic studies of adsorption of Cu2+ from aqueous solutions by Mg2+/K+ type orange peel adsorbents. J Hazard Mater 174:756
Liu Y, Liu YJ (2008) Biosorption isotherms, kinetics and thermodynamics. Sepa Purif Technol 61:229
Malik PK, Saha SK (2003) Oxidation of direct dyes with hydrogen peroxide using ferrous ion as catalyst. Sep Purif Technol 31:241
Mohapatra M, Khatun S, Anand S (2009) Kinetics and Thermodynamics of lead (II) adsorption on lateritic nickel ores of Indian origin. Chem Eng J 155(184–190):59
Munagapati VS, Kim DS (2016) Adsorption of anionic azo dye congo red from aqueous solution by cationic modified orange peel powder. J Mol Liquids 220:540
Mustafa TY, Sen TK, Afroze S, Ang HM (2014) Dye and its removal from aqueous solution by adsorption: A review. Adv Coll Inter Sci 209:172
Myers R, Khuri A, Carter W (1989) Adsorption of anionic response surface methodology: 1966–1988. Technometrics 31(2):137–157
Namasivayam C, Sureshkumar MV (2006) Anionic dye adsorption characteristics of surfactant modified coir pith, a waste lignocellulosic polymer. J Appl Polym Sci 100:1538
Ndazi BS, Nyahumwa C, Tesha J (2007) Chemical and Thermal stability of Rice husks against alkali Treatment. BioResources 3(4):1267
Niraj N, Pandey KM, Dey A (2018) Tribological behaviour of Magnesium Metal Matrix Composites reinforced with fly ash cenosphere. Mater Today: Proc 5(9):20138
Onal Y (2006) Kinetics of adsorption of dyes from aqueous solution using activated carbon prepared from waste apricot. J Hazard Mater B137(3):1719–1728
Panswad T, Wongchaisuwan S (1986) Mechanisms of dye wastewater colour removal by magnesium carbonate-hydrated basic. Water Sci Technol 18:139
Rahman M, Dey A, Pandey KM (2018) Machinability of cenosphere particulate–reinforced AA6061 aluminium alloy prepared by compocasting. Proc Inst Mech Eng Part B: J Eng Manuf 232(14):2499
B. Railsback (2006) Some fundamentals of mineralogy and geochemistry. Dept Geology, Univ. of Georgia, Athens, GA.
Rajoriya S, Saharan VK, Pundir AS, Nigam M, Roy K (2021) Adsorption of methyl red dye from aqueous solution onto eggshell waste material: Kinetics, isotherms and thermodynamic studies. Curr Res Green Sustain Chem 4:100180
Ravikumar K, Deebika B, Balu K (2005) Decolourization of aqueous dye solutions by a novel adsorbent: Application of statistical designs and surface plots for the optimization and regression analysis. J Hazar Mater 122:75
Ravikumar K, Krishnan S, Ramalingam S (2007) Optimization of process variables by the application of response surface methodology for dye removal using a novel adsorbent. Dye Pigm 72:66
Reddy DHK, Yun YS (2016) Spinel ferrite magnetic adsorbents: alternative future materials for water purification. Coord Chem Rev 315:90
Romdhane DF, Satlaoui Y, Nasraoui R, Charef A, Azouzi R (2020) Adsorption, modeling, thermodynamic, and kinetic studies of methyl red removal from textile-polluted water using natural and purified organic matter rich clays as low-cost adsorbent. J Chem 2020:17
RSM TDMKPS (2014) Removal of methyl red from aqueous solution by adsorption on treated banana pseudostem fibers using response surface method (rsm). Malays J Anal Sci 18(3):592–603
Saeed A, Sharif M, Iqbal M (2010) Application potential of grapefruit peel as dye sorbent: kinetics, equilibrium and mechanism of crystal violet adsorption. J Hazar Mater 179:564
Su Y, Zhao B, Xiao W, Han R (2013) Adsorption behaviour of light green anionic dye using cationic surfactant modified what straw in batch and column mode. Environ Sci Pollut Res 20:5558
Tarawou T, Horsfall M Jr, Vicente JL (2007) Adsorption of methyl red by water-hyacinth (eichornia crassipes) biomass. Chem Biodivers 4(9):2236–2245
Taweel TA (2009) Multi-response optimization of EDM with Al-Cu-Si-TiC P/M composite electrode. Int J Adv Manuf Technol 44:100
Taweel TL, Gouda SA (2010) Performance analysis of wire electrochemical turning process–RSM approach. Int J Adv Manuf Technol 53:18
Vadiveloo J, Nurfariza B, Fadel JG (2009) Natural improvement of Rice husk. Animal Feed Sci Technol 151:299
Vankar PS (2000) Chemistry of natural dyes. Resonance 5:73–80
Webi TW, Chakravorty RK (1974) Pore and solid diffusion models for fixed-bed adsorbents. AICHE J 20:228
Yagub MT, Sen TK, Ang H (2012) Equilibrium, kinetics, and thermodynamics of methylene blue adsorption by pine tree leaves. Water Air Soil Pollut 223:67
Zhou T, Lu W, Liu L, Zhu H, Jiao Y (2015) Effective adsorption of light green anionic dye from solution by CPB modified peanut in column mode. J Mol Liq 211:909
Zhu CS, Wang LP, Chen WB (2009) "Removal of Cu (II) from aqueous solution by agricultural by product: peanut hull. J of Hazardous Materials 168:739–746
Zubair M, Aziz HA, Ihsanullah I, Ahmad MA, Al-Harthi MA (2021) Biochar supported CuFe layered double hydroxide composite as a sustainable adsorbent for efficient removal of anionic azo dye from water. Environ Technol Innov 23:101614
Zubair M, Aziz HA, Ihsanullah I, Ahmad MA, Al-Harthi MA (2022) Enhanced removal of eriochrome black T from water using biochar/layered double hydroxide/chitosan hybrid composite: Performance evaluation and optimization using BBD-RSM approach. Environ Res 209:112861